J Mater Sci (2008) 43:4561–4566
DOI 10.1007/s10853-008-2638-6

Texture simulation of aluminum rod during equal channel angular pressing

Majid Hoseini · Mahmood Meratian · Hualong Li · Jerzy A. Szpunar

Received: 12 January 2008 / Accepted: 7 April 2008 / Published online: 17 April 2008

Abstract A general procedure for texture simulation in multi-pass equal channel angular pressing (ECAP) with capability of applying different processing routes is proposed. The program inputs are the initial texture and the loading condition and the output is texture after deformation. Deformation texture in ECAP of aluminum rod was predicted based on simple shear model for deformation and Visco plastic self consistent model for texture simulation. The simulation was done for two consecutive passes of ECAP and the results were compared with experimental texture measurements. The initial texture of the sample before ECAP was found to play a key role in formation of the final texture and a good agreement between the simulated and the experimental texture was obtained.

Introduction

Severe plastic deformation (SPD) techniques have been widely used in recent years with the aim of producing sub-micron and nanostructured polycrystalline materials with superior mechanical properties [1]. In these techniques, very high plastic strain can be applied to solid bulk materials without any significant changes in the specimen's overall dimensions. Equal channel angular pressing (ECAP) is one of the SPD processing techniques which was first introduced by Segal [2] in the early 70s but extensive works have been done on this process from the 90s [3]. In ECAP process, bulk solid rod or bar is pressed trough a die consisting of two channels having a constant cross section meeting each other at an abrupt bent through a certain angle Φ (usually close to 90° or 120°). This bending angle is an important parameter in the process [1–3]. Microstructure and grain size are changed during ECAP as a result of large plastic deformation that takes place in a narrow region at the intersection of two channels [4]. Like in other SPD techniques, since the material's cross section shape and size remain the same, ECAP process can be repeated several times. High plastic strain can then be applied to the material. Rotation of billet (processing routes) between passes is another key parameter in ECAP process [5]. In general, deformation mechanisms in ECAP depend on material properties and processing parameters. For a specific material, number of passes (amount of induced strain), die angle (Φ), and the processing routes are controllable and can widely affect the deformation process and microstructure [3–5]. Large plastic deformation and frequent changes in strain paths result in complex changes in microstructure and crystallographic texture of material. Texture investigation is an essential way to understand the deformation mechanism and grain refinement during this process [1].

Many investigations have shown that texture developed during ECAP is almost compatible with the texture obtained by other deformation processes like torsion, which are characterized by simple shear [3, 6–10]. Segal proposed a simple shear model for deformation mechanism during ECAP [4]. Computer modeling of the developed texture during ECAP has been also the matter of interest in recent studies. Gholinia et al. [9] used

M. Hoseini (✉) · H. Li · J. A. Szpunar
Department of Mining, Metals and Materials Engineering, McGill University, Montreal, QC, Canada H3A 2B2
e-mail: majid.hoseini@mcgill.ca

M. Hoseini · M. Meratian
Department of Materials Engineering, Isfahan University of Technology, Isfahan 84156-83111, Iran

computer simulation based on a Taylor model [11] to simulate the deformation texture after several passes. They considered two different die angles (90° and 120°) regardless of the rotation of billet. Li et al. [12–15] in systematic progressive investigation used texture simulation to evaluate the effect of processing parameters and also to improve deformation texture modeling in different materials. They compared the results for simple shear, fan shape [16], and finite element models to simulate plastic deformation. They implemented Visco plastic self consistent (VPSC) [11, 17] and Taylor models for texture simulation obtained from deformation.

In this paper a general procedure for the texture simulation during ECAP is proposed. The procedure has the capability to simulate texture after a multi-pass process. All process routes may be applied as well. Furthermore, experimentally measured textures could be used as an input data based on which all the above-mentioned models can be applied. This procedure was used to predict the texture of pure aluminum on subsequent passes. Simple shear deformation model and VPSC texture model were then applied. The simulated results with different initial texture inputs were compared with experimental X-ray texture measurement results.

Experimental

Commercially pure aluminum was received in the form of extruded rod, 12.7 mm in diameter and chemical composition of Al—0.11%Si—0.46%Fe—0.12%Cu—0.01%Mn—0.02%Ti. Cylindrical samples with diameter of 12 mm were machined and cut into parts of 70 mm length which were then annealed at 400 °C for 2 h. The average grain size of the samples after annealing was about 70 μm. ECAP process was carried out using a $\Phi = 90°$ die with $\Psi = 20°$ outer arc of curvature. The samples were subjected to ECAP with carbon oil based lubricant at room temperature for one and two passes via route Bc (clockwise 90° rotation of the sample between two passes). The textures of the samples were measured in a cross-section cut from the middle of the specimens using SIEMENS DX-500 X-ray diffractometer. Orientation distribution functions (ODF) and pole figures were analyzed using TextTool software.

Modeling procedure

General model

ECAP process is shown schematically in Fig. 1. Simple shear deformation at the intersection plane of the channels

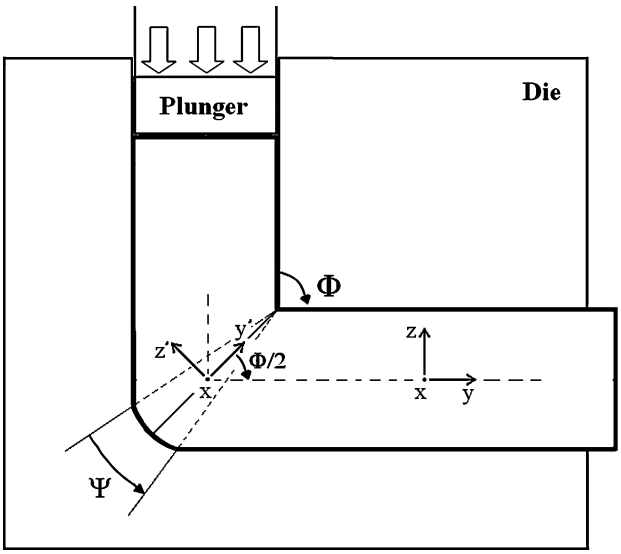

Fig. 1 Schematic of the ECAP process

is considered, as proposed by Segal [4]. Therefore two coordination systems for die geometry and the applied deformation were selected. Reference coordination system *xyz* corresponds to the die's exit channel. The *y*-axis is along the specimen's length and the texture is defined in the *xz* plane. Deformation coordination system $xy'z'$ includes shear deformation in the xy' plane along $-y'$ direction. The deformation plane is perpendicular to the *yz* plane and makes an angle of Φ/2 with *y* direction. Assuming *xz* plane (sample cross section) as a reference for measured and simulated textures, a model with respect to the *xyz* system is proposed for texture simulation in ECAP process. In this model (Fig. 2) the material flows along *y* direction and deformation is applied on it according to plastic deformation model. For example, in a simple shear model deformation occurs in the plane that is inclined by Φ/2° with respect to *xy* plane.

In each pass, simulation is conducted by applying deformation condition on the input texture data and the

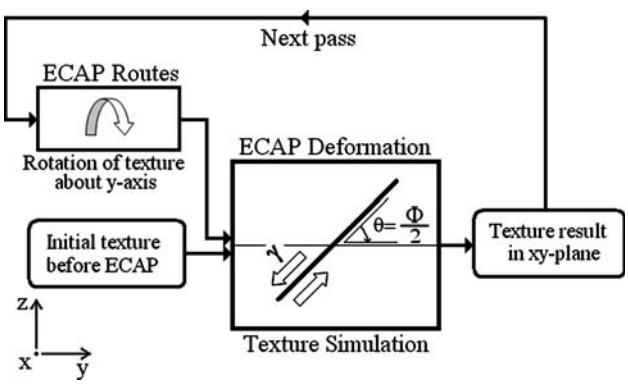

Fig. 2 Modeling procedure used for multi-pass texture simulation of ECAP process

output texture is predicted by using texture simulation models (VPSC or Taylor). The simulated output texture of each pass can be used as the input texture for the next pass. The texture in multi-pass ECAP could then be predicted. Sample rotation between consecutive passes (ECAP routes) could also be applied in this model by rotation of texture results around y-axis before using it as the input texture of the next pass.

In order to verify the model, a simple shear deformation was used for the deformation model, while other models like fan shape model or deformation data obtained from finite element simulation could also be applied.

Simulation with simple shear deformation

The magnitude of shear strain depends on the die's intersection angle (Φ) and the arc of outer corner (Ψ) in the intersection. This is formulated as in Eq. 1 [18].

$$\gamma = 2\cot\left(\frac{\Phi}{2}+\frac{\Psi}{2}\right) + \Psi\mathrm{cosec}\left(\frac{\Phi}{2}+\frac{\Psi}{2}\right) \quad (1)$$

The displacement gradient tensor in the $xy'z'$ system is shown by Eq. 2. The minus sign before γ indicates that the shear strain occurs in $-y'$ direction.

$$T_{xy'z'} = \begin{bmatrix} 0 & 0 & 0 \\ 0 & 0 & -\gamma \\ 0 & 0 & 0 \end{bmatrix} \quad (2)$$

As seen in Fig. 1, T_{xyz} in the xyz system can be derived by $\theta = \Phi/2$ clockwise rotation of $T_{xy'z'}$ around x-axis. Equation 3 shows the displacement gradient tensor of ECAP process in the xyz reference system.

$$T_{xy'z'} = \begin{bmatrix} 0 & 0 & 0 \\ 0 & \gamma\sin\theta\cos\theta & -\gamma\cos^2\theta \\ 0 & \gamma\sin^2\theta & -\gamma\sin\theta\cos\theta \end{bmatrix} \quad (3)$$

Texture simulation was carried out using a computer program based on VPSC model. In this model each grain is considered as an ellipsoidal visco-plastic inclusion interacting with effective media [11, 17]. The shape and orientation of the grains are characterized by the length and orientation of the ellipse main axes which can be mathematically described by the eigen values and eigen vectors of the displacement tensor.

General fcc structure with 12 slip system and constant critical resolved shear stress (CRSS) were assumed in the calculations. Texture results were calculated in ODF represented in xz plane of xyz system. The simulation of the first pass was run with the ODF of 5000 grains with random texture (created by TextTools program) as the initial texture before ECAP. Texture simulation was done for the first and second passes assuming $\Phi = 90°$ and $\Psi = 20°$ to compare with experiments.

Results and discussions

Texture results after one pass

The pole figures of simulated and measured texture after one pass ECAP are illustrated in Fig. 3. Texture results are represented as three pole figures ({111}, {200}, and {220}) projected on the plane perpendicular to the longitudinal axes of specimen at exit channel of ECAP die (xz plane). Position and intensity of the peaks in these three pole figures will be used to evaluate the accuracy of simulation results. Comparing the corresponding pole figures shows that the simulations could not match the experiments. The peaks in the simulated pole figures are quite lower (about half) than the experimental peaks. Although some of the peaks were simulated in the same positions as the measured peaks, at least one strong peak in each pole figure was predicted in a totally different position. For example in the {111} and {220} pole figures, one pair of measured peaks appeared as a single but wider peak at the middle position in simulated pole figure.

In the simple shear deformation texture, most important ideal orientations are claimed to be distributed along two fibers. The former has a crystallographic slip direction

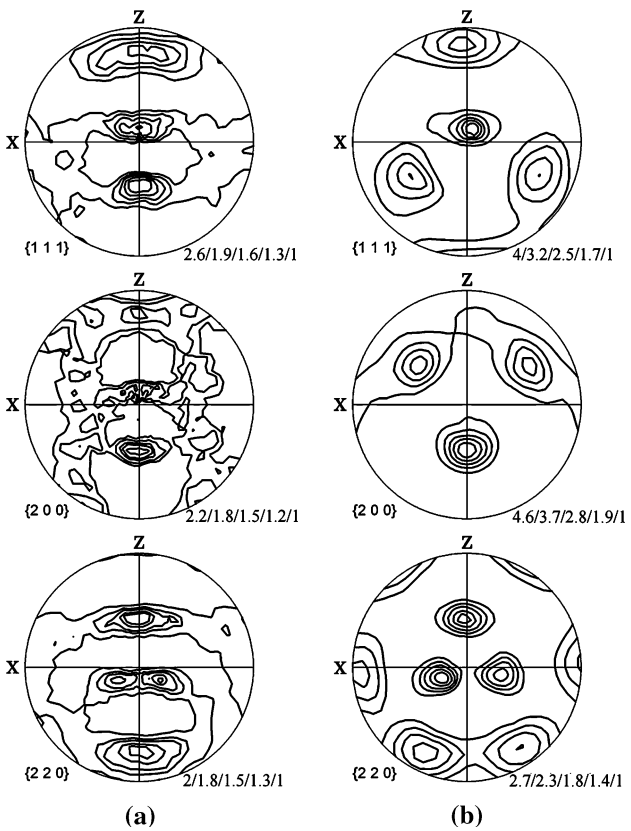

Fig. 3 Texture results showing pole figures of (**a**) simulated (**b**) X-ray measured aluminum rod, texture after 1 pass ECAP

parallel to shear direction and the latter has a crystallographic slip plane parallel to shear plane [19–21]. For the fcc materials {111}<110> is the slip system, so the <110>-fiber {hkl}<110> and the {111}-fiber {111}<uvw> would be the important texture fibers after shear deformation. Assuming simple shear deformation in xy' plane (ECAP process in Fig. 1), the Miller indices and positions of the main ideal orientations in {111} pole figure, projected on the $y'z'$ plane, are shown in Fig. 4a [13]. After 45° rotation of this pole figure around x and then 90° around z-axis, the {111} pole figure having ideal orientations position projected on xz plane is shown in Fig. 4b.

Considering Fig. 4b as the ideal reference for shear deformation in ECAP, the peaks in {111} pole figures in both the simulated and measured are showing ideal orientations. The notable difference is that in the simulated pole figure, the strongest peak is located in the conjunction of four different A orientations in lower hemisphere of the pole figure, while in the measured one, all the peaks are located around the C orientations.

The simulated results shown in Fig. 3a are in good agreement with the results found in the literature [8, 9, 13–15] for fcc metals processed under similar conditions. Initial texture may account for differences between the simulated and the measured textures, since during simulation a polycrystalline model with a random texture was used as the initial texture. On the other hand researchers have shown that in fcc metals with high stacking fault energy like aluminum, deformation textures after shear strain are typically represented as a <110>-fiber with less strong {111}-fiber. This means that shear strain causes tendencies for the slip direction to become aligned with the shear direction. Research has also shown that in

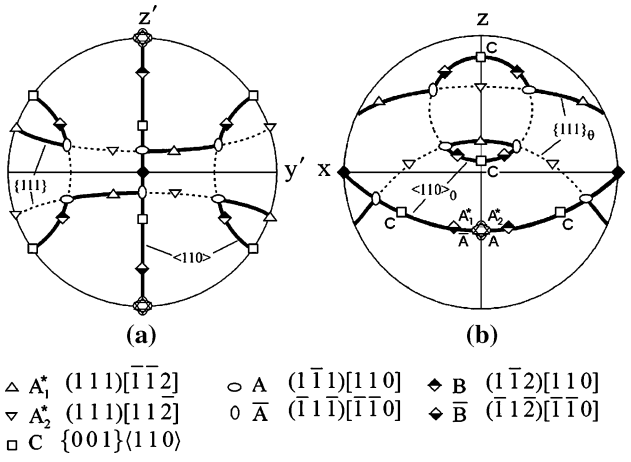

Fig. 4 {111} Pole figures showing {111}-fiber, <110>-fiber, and ideal orientations after simple shear deformation in fcc materials. (**a**) In $xy'z'$ system where the simple shear has occurred in xy' plane along $-y'$ direction. (**b**) In xyz system derived from $xy'z'$ system

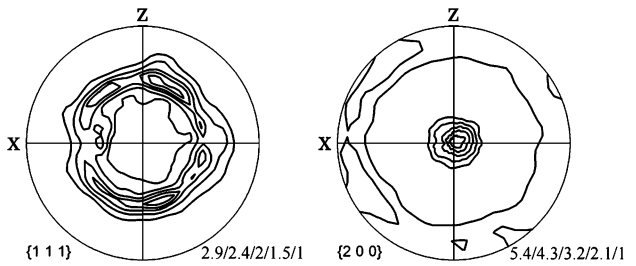

Fig. 5 {111} and {200} pole figures measured from aluminum specimen before ECAP

aluminum, the ideal {100}<110> component (C position) has the highest orientation density on the <110>-fiber [11, 21]. It means that the high stacking fault energy of aluminum may also cause the differences between the measured and simulated results because in the simulation, simple fcc crystal with {111}<110> slip system was used regardless of the possible influence of the stacking fault energy.

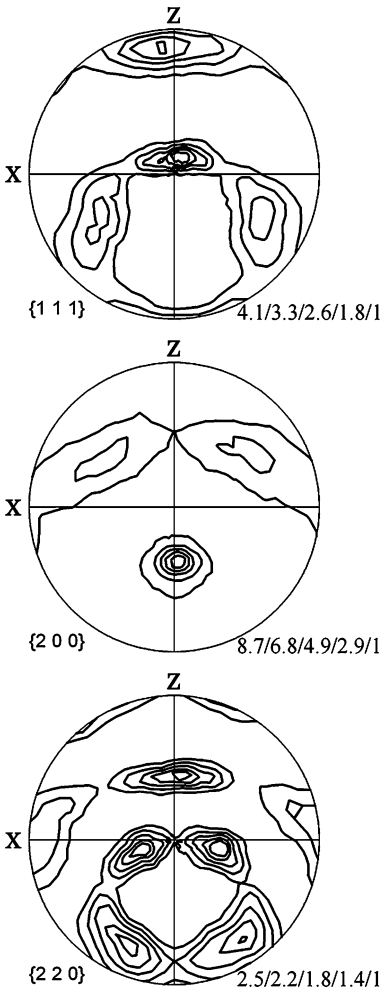

Fig. 6 Pole figures after one pass simulated by using experimental measured texture of Al rod before ECAP as the input for simulation

Effect of the initial texture

The {111} and {200} pole figures of the initial texture measured from the cross section of specimen before ECAP are shown in Fig. 5. The initial texture shows a {200} fiber texture parallel to the longitudinal axes of the specimen.

Figure 6 shows the results which were obtained from simulation using actual measured texture as the input. These pole figures have a good similarity to the measured textures in Fig. 3b, such that almost all the peaks were predicted in the right positions with the similar intensities, except only in {200} pole figure where the maximum intensity of the peaks obtained from the simulation is around two times higher than the measured pole figure. This is probably caused by relatively strong {200} fiber texture existing in the initial texture. It is also worth to point out small differences in the peak's shape in corresponding pole figures. For example, in the measured {111} pole figure the peaks are extended along the <110>-fiber (in reference to Fig. 4b), while in the simulated one, peaks are extended along the (111)-fiber. High stacking fault energy in aluminum and the tendency of this metal to show the <110>-fiber more than {111}-fiber after simple shear could cause the above differences in the peak's shape.

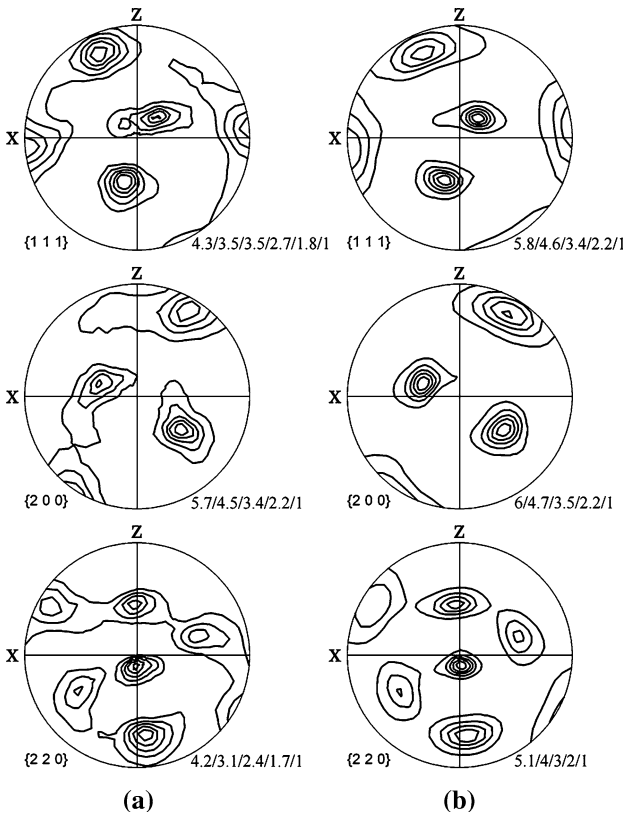

Fig. 7 Texture results showing pole figures of (**a**) simulation with experimental initial texture and (**b**) X-ray measured aluminum rod texture after two passes of ECAP using route Bc

Texture results after two passes

Figure 7 shows the texture results after two passes of ECAP using route Bc. Since in the route Bc the specimen rotates 90° between two passes, significant changes occurred in texture during the second pass. Two sets of pole figures including measured and simulated textures are shown in this picture. Real measured initial texture was used as the input data for the first pass simulation. The second pass simulation used results of the first pass simulation as the input data. Measured and simulated textures fit perfectly regarding positions and intensities of the peaks. The maximum difference is seen in the texture strength of the {111} pole figures, where the maximum intensity in the simulated pole figure is about 25% less than the measured one. The match between measured and simulated pole figures after the second pass shows that the simulation model has predicted well the experimental results.

Conclusions

Deformation texture of aluminum rod after two passes of ECAP was successfully predicted using a general procedure proposed for computer simulation in this process. The initial texture of aluminum rod before ECAP must be used in the simulation. When an unrealistic random input texture was used, the differences between the experimental and the simulated textures were significant. Although simple shear model was adopted for deformation, the effectiveness of the proposed procedure was proved by excellent agreement between texture results from experiments and simulation after one and two passes.

References

1. Valiev RZ, Islamgaliev RK, Alexandrov IV (2000) Progr Mater Sci 45:103. doi:10.1016/S0079-6425(99)00007-9
2. Segal VM, Drobyshevski AE, Kopylov VI (1981) Russ Metal (Eng trans) 1:99
3. Valiev RZ, Langdon TG (2006) Progr Mater Sci 51:881. doi:10.1016/j.pmatsci.2006.02.003
4. Segal VM (1995) Mater Sci Eng A 197:157. doi:10.1016/0921-5093(95)09705-8
5. Nakashima K, Horita Z, Nemoto M, Langdon TG (2000) Mater Sci Eng A 281:82. doi:10.1016/S0921-5093(99)00744-3
6. Suwas S, Toth LS, Fundenberger J-J, Eberhardt A, Skrotzki W (2003) Scr Mater 49:1203. doi:10.1016/j.scriptamat.2003.08.011
7. Suh J-Y, Han J-H, Oh K-H, Lee J-C (2003) Scr Mater 49:185. doi:10.1016/S1359-6462(03)00208-2
8. Beyerlein IJ, Lebensohn RA, Tome CN (2003) Mater Sci Eng A 345:122. doi:10.1016/S0921-5093(02)00457-4

9. Gholinia A, Bate P, Prangnell PB (2002) Acta Mater 50:2121. doi:10.1016/S1359-6454(02)00055-1
10. Huang WH, Chang L, Kao PW, Chang CP (2001) Mater Sci Eng A 307:113. doi:10.1016/S0921-5093(00)01881-5
11. Kocks UF, Tome CN, Wenk HR (2000) Texture and anisotropy. Cambridge University Press, Cambridge
12. Li S, Gazder AA, Beyerlein IJ, Pereloma EV, Davies CHJ (2006) Acta Mater 54:1087. doi:10.1016/j.actamat.2005.10.042
13. Li S, Beyerlein IJ, Bourke MAM (2005) Mater Sci Eng A 394:66. doi:10.1016/j.msea.2004.11.032
14. Li S, Beyerlein IJ, Alexander DJ, Vogel SC (2005) Acta Mater 53:2111
15. Li S, Beyerlein IJ, Alexander DJ, Vogel SC (2005) Scr Mater 52:1099. doi:10.1016/j.scriptamat.2005.02.008
16. Segal VM (2003) Mater Sci Eng A 345:36. doi:10.1016/S0921-5093(02)00258-7
17. Lebensohn RA, Tome CN (1993) Acta Metall Mater 41:2611. doi:10.1016/0956-7151(93)90130-K
18. Iwahashi Y, Wang J, Horita Z, Nemoto M, Langdon TG (1996) Scr Mater 35:143. doi:10.1016/1359-6462(96)00107-8
19. Toth LS, Gilormini P, Jonas JJ (1988) Acta Metall 36:3077. doi:10.1016/0001-6160(88)90045-4
20. Montheillet F, Cohen M, Jonas JJ (1984) Acta Metall 32:2077. doi:10.1016/0001-6160(84)90187-1
21. Canova GR, Kocks UF, Jonas JJ (1984) Acta Metall 32:211. doi:10.1016/0001-6160(84)90050-6